HHS Public Access

Author manuscript

Nat Chem Biol. Author manuscript; available in PMC 2014 October 01.

Published in final edited form as:

Nat Chem Biol. 2014 April ; 10(4): 286–290. doi:10.1038/nchembio.1477.

Dissecting signaling through activation of specific Src-effector complexes *in vivo*

A.V. Karginov[1,2], **D. Tsygankov**[1], **M. Berginski**[3], **P.-H. Chu**[1], **E.D. Trudeau**[1], **J.J. Yi**[1], **S. Gomez**[3], **T.C. Elston**[1], and **K.M. Hahn**[1,4,*]

[1]Department of Pharmacology, University of North Carolina at Chapel Hill

[2]Current address: Department of Pharmacology, University of Illinois at Chicago

[3]Department of Biomedical Engineering, University of North Carolina at Chapel Hill

[4]Lineberger Cancer Center, University of North Carolina at Chapel Hill

Abstract

We describe an approach to selectively activate a kinase in a specific protein complex or at a specific subcellular location within living cells, and within minutes. This reveals the effects of specific kinase pathways without time for genetic compensation. The new technique, dubbed RapRTAP (rapamycin regulated targeted activation of pathways) was used to dissect the role of Src kinase interactions with FAK and p130Cas in cell motility and morphodynamics. The overall effects of Src activation on cell morphology and adhesion dynamics were first quantified, without restricting effector access. Subsets of Src induced behaviors were then attributed to specific interactions between Src and the two downstream proteins. Activation of Src in the *cytoplasm* versus at the cell membrane also produced distinct phenotypes. The conserved nature of the kinase site modified for RapRTAP indicates that the technique can be applied to many kinases.

Introduction

Protein kinases regulate cell behaviors by activating multiple downstream pathways in parallel. Downstream players act synergistically, controlling different aspects of the cellular machinery, so the role of specific kinase interactions is difficult to decipher. Small molecule kinase inhibitors affect all pathways downstream of the kinase, and often cannot target one kinase among similar isoforms. Genetic manipulations are prone to cell compensation and provide only poor temporal resolution. None of these methods couple the ability to activate a specific kinase with the ability to restrict kinase interaction to one downstream target.

*Correspondence to: khahn@med.unc.edu.

Author Contributions. AK and KH initiated the project, and AK carried out the bulk of the experimental studies. DT and TE developed and applied the new method used to analyze filopodia dynamics. MB and SG quantified cell adhesion dynamics. All other morphodynamic quantitations were by DT and AK. ET and PHC assisted with kinase assays and cloning. JY provided mCherry-stargazin. All authors contributed to the writing of the manuscript.

Competing Financial Interests: The authors declare no competing financial interests.

Src is a ubiquitous protein important in a wide array of cell behaviors[1], including normal motility and metastasis[1-3], but little is known about the immediate effects of Src activation, or which downstream molecules mediate which Src effects. Src regulates multiple cellular processes by signaling in different protein complexes and at different subcellular locations. Membrane targeting via N-terminal myristoylation of Src is required for Src-mediated oncogenic transformation and normal motility, but there is a substantial pool of Src in the cytoplasm, whose role remains unknown[4-9]. This cytosolic Src can potentially interact with proteins important for morphodynamics, at focal adhesions or the cytoskeleton[10]. In this study we examines specific effects of Src signaling through focal adhesion kinase (FAK) and p130Cas, to control cell morphology and migration[3, 11, 12]. Both interactions are known to play a role in motility, but the specific events triggered by each remained obscure.

To rapidly activate a kinase in complex with a single specific target, we built upon our previously described RapR approach for kinase activation[13, 14]. RapR kinases are made by inserting a modified FK506-binding protein (iFKBP) into a highly conserved portion of the kinase catalytic domain, inactivating the kinase. Addition of rapamycin leads to heterodimerization of the inserted iFKBP with a coexpressed FKBP12-rapamycin binding domain (FRB), causing kinase reactivation. While valuable, this approach leads to interaction of the kinase with all downstream targets indiscriminately. Here, by fusing a modified FRB to a specific kinase target, activation was restricted to that kinase-target interaction alone (Fig. 1a). The new technique, dubbed RapR-TAP (Rapamycin-Regulated Targeted Activation of Pathways) enabled us to dissect the role of Src interactions with specific downstream effectors or, by localizing the FRB, compare effects of Src activation at different subcellular locations.

Results

Morphological changes stimulated by the activation of Src

Using a rapamycin-inducible Src (RapR-Src)[13], we first characterized the cell activities produced simply by Src activation, without directing Src to specific targets. These behaviors could later be compared with those produced when RapRTAP was to restrict Src activation to specific protein complexes or subcellular locations. To ensure that Src was activated only by rapamycin, and not subject to upstream regulation, we used the Y529F mutant[15] of the RapR-Src construct. Activation of RapR-Src in HeLa cells led to cell spreading, an increase in the number and length of filopodia, and an increase in the number of adhesions accompanied by adhesion elongation (Fig. 1b-d, Supplementary Results, Supplementary Movies 1-4). Spreading was quantified as the total change in cell area, and protrusive activity as the sum of the areas associated with regions of the cell that undergo local extensions between subsequent movie frames (Supplementary Fig. 1). Adhesion number and shape were assessed using a previously published method[16]. To quantify filopodia dynamics, we applied a computational method that allows accurate identification and tracking of all cellular protrusions of arbitrarily complex shape (Supplementary Fig. 2). The method, which represents the cell boundary as a tree graph, allows unambiguous specification of filopodia and, importantly, works for cells and protrusions of any scale and geometry in an unbiased automated manner (see methods).

All quantified changes began within 2-4 minutes of Src activation (Supplementary Fig. 3-5). The area of the HeLa cells increased 25-30% (Supplementary Fig. 3a). Area increase was produced by a transient burst of protrusive activity that subsided after roughly 40 minutes (Supplementary Fig. 3b). Filopodia increased 2-3 fold in density along the cell edge and grew roughly 50% longer. These changes plateaued after roughly 20 minutes (Supplementary Fig. 4). Adhesions increased in number by 80% and became more filamentous and elongated (Supplementary Fig. 5). The change in adhesion number coincided with the period of rapid cell spreading. Control studies showed that these changes were specifically due to Src activity. The kinase inactive mutant of RapR-Src (D388R) did not produce any significant change in cell area, protrusive activity or filopodia (Supplementary Fig. 3-5). Similarly, no effects were observed in cells that were not transfected with any Src constructs (Supplementary Fig. 3-4).

A series of controls ensured that the effects we observed were solely due to RapR-Src: Activation of RapR-Src with rapamycin increased the phosphorylation of the Src substrates paxillin, p130Cas and FAK, and to robust autophorylation of RapR-Src on Tyr418, a known indicator of Src activation[1, 15] (Supplementary Figs. 6 and 7). Rapamycin produced little or no Tyr418 phosphorylation of endogenous Src (Supplementary Fig. 6). Cells not expressing RapR-Src or expressing kinase-inactive RapR-Src showed no significant change in phosphorylation of paxillin, p130Cas, FAK or endogenous Src Tyr418 upon rapamycin treatment. Expression of kinase inactive RapR-Src did not significantly affect the expression level or Tyr418 phosphorylation of endogenous Src. (Supplementary Fig. 6). Localizations of active and inactive RapR-Src were like those previously described for wild type Src[10, 17, 18] (Supplementary Fig. 8). Rapamycin was not added until the cells had already reached their maximum area during normal plating, indicating that Src activity alone was sufficient to promote additional spreading.

Membrane versus cytoplasmic Src activation

To parse out the roles of Src that require membrane translocation, we mutated RapR Src to eliminate the myristoylation required for membrane binding (G2A mutant)[19], then compared activation using either soluble cytosolic FRB, or FRB anchored to the membrane by the Src N-terminal myristoylation domain (N terminal 11 aa[20], Fig. 2a). The G2A mutation of RapR-Src did not affect its catalytic activity (Supplementary Fig. 9).

Activation of Src targeted to the plasma membrane led to robust spreading, as shown by a burst of protrusive activity and corresponding increase in cell area even greater than that seen upon activation of Src alone (Fig. 2b-d, Supplementary Movie 5, Supplementary Fig. 10, 11). Surprisingly, Src activated without membrane anchoring was also able to induce protrusive activity, but, in contrast to membrane-anchored Src, protrusive activity never ceased and activation did not lead to an increase in cell area (Fig. 2b-d, Supplementary Movie 6, Supplementary Fig. 10, 11). Only the membrane-anchored Src was able to produce a substantial increase in adhesion number (Fig. 2e, Supplementary Fig. 12), suggesting feedback in which protrusive activity is halted when adhesion formation leads to stable protrusions. Filopodia production required Src membrane localization, suggesting different pathways for lammelipodial versus filopodial protrusion (Fig. 2f, g, Supplementary Fig. 13,

14). Focal adhesion shape changes were produced only by activation of nonmyristoylated Src (Fig. 2h, Supplementary Fig. 15).

RapRTAP analogs of FAK and p130Cas

To examine the role of Src interactions in morphodynamics, we needed to be sure that Src interactions relevant to morphodynamics could only occur through our addition of rapamycin. We therefore examined the effects of mutations in the Src SH2 domain (R175L) and SH3 domain (W118A), to better understand downstream protein interactions and eliminate the ability of RapR Src to induce morphodynamics. Mutation of the SH2 domain alone eliminated all of the effects we had observed when simply activating Src (Supplementary Fig. 16-21), while mutation of the SH3 domain was only partially effective (Supplementary Fig. 16-21). Src phosphorylation of paxillin, which interacts with the Src SH3 domain, occurred at reduced levels even after the Src SH2 R175L mutation, but this was not sufficient to produce quantifiable phenotypes (Supplementary Fig. 6, 22). Control studies showed that neither the SH2 nor the SH3 mutations affected catalytic activity (Supplementary Fig. 9).

Having learned that Src interactions mediated through its SH2 domain are critical for induction of morphological changes, we decided to focus on proteins whose interactions are mediated by this domain, specifically FAK and p130Cas. Mutation of the p130Cas sites phosphorylated by Src have clear effects on cell motility[12], and the Src-FAK interaction is known to be important for regulating cell adhesion dynamics[3, 11].

To generate RapR-TAP analogs for Src-FAK and Src-p130Cas, we created chimeras of FAK and p130Cas wherein the binding site for the Src SH2 domain was replaced by the FRB domain (insertion at FAK Tyr397[21] and p130Cas Tyr668[22]). Addition of rapamycin would lead to activation of RapR-Src(R175L) only when it was interacting withthe modified FAK or p130Cas (Fig. 3a). The RapR-Src R175L mutation prevented interaction with endogenous binding partners. Assays based on co-expression of RapR-Src with either FAK-FRB or p130Cas-FRB, followed by immunoprecipitation and Western blotting, showed that RapR Src was activated when in complex with FAK-FRB or p130Cas-FRB; rapamycin induced a robust increase in FAK-FRB and p130Cas-FRB tyrosine phosphorylation (Supplementary Fig. 23). The modifications of p130Cas and FAK did not affect their subcellular localization (Supplementary Fig. 24). Activation of RapR-Src(R175L) led to robust RapR-Src autophosphorylation, and had no effect on the autophosphorylation of endogenous Src (Supplementary Fig. 22). RapR-Src (R175L) alone was unable to change the phosphorylation of endogenous FAK or p130Cas (Supplementary Fig. 25). Previous studies indicate that phosphorylation of p130Cas occurs downstream of Src-FAK interaction[23]. Indeed, we saw phosphorylation of endogenous p130Cas in response to activation of the Src-FAK complex, while formation of Src-p130Cas did not lead to phosphorylation of endogenous FAK (Supplementary Fig. 25).

Dissecting the roles Src-FAK and Src-p130Cas

With the RapRTAP analogs of p130Cas and FAK in hand, we could differentiate the roles of each protein in Src-induced morphodynamics. Expression of RapR-Src(R175L) with

either p130Cas-FRB or FAK-FRB produced different subsets of the behaviors induced simply by Src activation: Src complexed with p130Cas, but not with FAK, generated filopodia and increased their length (Fig. 3b, c, Supplementary Fig. 26, 27). The Src-p130Cas complex was also much more effective at increasing adhesion number than was the Src-FAK complex (Fig. 3d, Supplementary Fig. 28). In contrast, Src-p130Cas had little effect on adhesion morphology, while Src-FAK produced an exaggerated version of the adhesion elongation that had been produced by Src alone. Adhesions became long and wispy, with less distinct borders. These adhesions were difficult to segment using automated image analysis, so naïve observers were asked to score movies for adhesion morphology. (Fig. 3e-g, Supplementary Movie 7). Both Src-FAK and Src-p130Cas generated cell spreading, but only p130Cas produced the limited burst of protrusion seen upon simple Src activation (Fig. 3h-j, Supplementary Fig. 29-31). FAK activation led to slower spreading and prolonged protrusive activity.

Discussion

We first used RapR Src for simple activation of Src, allowing it to interact with multiple effectors. Morphological changes triggered specifically by Src are frequently studied using overexpression of constitutively active Src mutants, but this can only reveal phenotypes that occur after prolonged exposure to elevated Src activity. RapR-Src revealed morphological changes occurring within minutes after activation, before genetic compensation could occur, and provided essentially absolute specificity, unlike drug treatments. RapR Src activation demonstrated that Src alone is sufficient to drive both lamellipodia and filopodia formation, and that it alone is capable of coordinating membrane protrusion and focal adhesions during cell spreading.

Next, RapRTAP was used to target Src activation to the cytoplasm versus the plasma membrane, suggesting a mechanism for coordination of Src-induced protrusion and adhesion. Src could generate protrusions even without membrane anchoring, but these protrusions did not cease even after prolonged activation, and did not result in stable spreading. In contrast, membrane-anchored Src did lead to spreading, and was required for formation of new adhesions. This suggests that Src drives protrusion until adhesions are formed; these adhesions then inhibit further Src-induced protrusions and stabilize nascent adhesions. This mechanism is consistent with previous studies showing coordination of adhesion dynamics and protrusion at the leading edge[24].

Finally, RapRTAP clearly differentiated cell behaviors induced by Src complexation with FAK or with p130Cas, leading to a model of the potential synergy between these two interactions (Fig. 4). The ability to activate a kinase while restricting activity to a specific target enables dissection of phenotypes produced by specific interactions and, as in our demonstration that the Src-FAK complex leads to phosphorylation of endogenous p130Cas, can be used to examine whether downstream events are the result of direct or indirect interactions with upstream proteins. Normal spreading was produced only through Src-p130Cas signaling. Also, only the p130Cas interaction could produce both protrusions and new adhesions to stabilize these protrusions (Fig. 4). When Src-FAK activation generated protrusions (with minimal adhesion formation) protrusive activity did not cease, suggesting

that signals from the new adhesions might inhibit further protrusion. Once adhesions are formed, FAK but not p130Cas was shown to play a role in adhesion maturation.

Src produced filopodia via a pathway that required p130Cas but not FAK (Fig. 4), demonstrating for the first time that Src can stimulate filopodia through p130Cas. p130Cas but not FAK has been shown to localize to the tips of filopodia[25], suggesting that p130Cas may mediate recruitment of Src for filopodia formation. Direct interaction of Src and p130Cas is likely required for filopodia formation; we demonstrated that Src-FAK activation leads to phosphorylation of endogenous p130Cas, but this was not sufficient to produce filopodia.

In summary, we have described an approach to activate specific kinase-induced signaling pathways in living cells (RapRTAP), combining rapid and specific kinase activation with targeted protein interaction or targeted subcellular localization. It revealed different roles for Src-FAK and Src-p130Cas protein complexes in early stages of Src-induced morphodynamics. Structural studies of RapR kinases indicate that this will be a broadly applicable approach[13, 26], capable of dissecting multiple kinase signaling networks *in vivo*.

Online Methods

Data analysis

Data in figures 1 through 3 are smoothed by running average using a Gaussian filter. The unsmoothed data, with error bars, are provided in the supplemental materials Statistical analysis of the data is also provided in supplementary materials

Antibodies and reagents

Anti-phospho-paxillin (Tyr31), anti-phospho-Src (Tyr418) and anti-phospho-FAK (Tyr397) antibodies were purchased from Invitrogen. Anti-GFP antibodies were purchased from Clontech. Anti-phosphotyrosine (4G10), anti-myc antibodies and IgG-coupled agarose beads were purchased from Millipore. Anti-p130Cas, anti-phospho-p130Cas (Tyr410), anti-FAK and anti-Src antibody were purchased from Cell Signaling Technology. Anti-paxillin antibody were a gift from Dr. Michael Schaller. Rapamycin was purchased from LC Laboratories. All restriction enzymes were purchased from New England Biolabs.

Molecular biology

GFP-paxillin, mCherry-paxillin, GFP-FAK, mCherry-FAK, RapR-Src-myc, mCherry-FRB and GFP-FRB constructs were previously described [13]. To generate pmVenus-p130Cas, the p130Cas gene was cut out of a pEBG-p130Cas plasmid (purchased from AddGene, provided by Dr. Raymond Birge) using BamHI and NotI, and then ligated with pmVenus-CI vectors predigested with BglII and PspOMI. RapR-Src-Cerulean-myc and RapR-Src-GFP-myc constructs were generated by insertion of GFP and Cerulean genes into the RapR-Src-myc construct using a modification of site-directed mutagenesis as previously described[14]. The mVenus-FAK construct was generated by replacing the GFP in the GFP-FAK construct with mVenus using a modification of site-directed mutagenesis as previously described[13, 14]. mVenus-FAK-FRB and mVenus-p130Cas-FRB constructs were generated by insertion of

FRB into mVenus-FAK (replacing Tyr397 codon) and mVenus-p130Cas (replacing Tyr668 codon) using a modification of site-directed mutagenesis as previously described[13, 14]. Myristoylated mCherry-FRB and GFP-FRB constructs were generated by insertion of myristolation N-terminal fragment of Src (encoding first 11 amino acids) at the N-term of mCherry and GFP in mCherry-FRB and GFP-FRB, using a modification of site-directed mutagenesis as previously described[13, 14]. G2A, W118A, R175L and Y529F mutations of RapR-Src were performed using a site directed mutagenesis method (QuikChange site-directed mutagenesis protocol, Agilent Technologies). To generate the stargazin-mCherry construct, the stargazin gene was PCR amplified from mouse stargazin cDNA and ligated into pmCherry-N1 using XhoI and BamHI sites. A multiple cloning site was also introduced into the intracellular loop of stargazin through PCR.

Cell imaging

Cells were plated on fibronectin-coated coverslips (5 mg/L fibronectin) 2-4 hours prior to imaging, then transferred into L-15 imaging medium (Invitrogen) supplemented with 5% fetal bovine serum. Live cell imaging was performed in an open heated chamber (Warner Instruments) using an Olympus IX-81 microscope equipped with an objective-based total internal reflection fluorescence (TIRF) system and a PlanApo N 60x TIRFM objective (NA 1.45) or a UPlanFLN 40X (Oil, NA 1.30) objective. All images were collected using a Photometrix CoolSnap ES2 CCD camera controlled by Metamorph software. A 440nm laser from Kimmon Koha (Ik Series He-Cd, model IK4171I-G), 491nm laser from Olympus (Cell TIRF 491 laser, model LAS/491/50) and 594nm laser from Cobolt (model Mambo) were used for TIRF imaging. Epifluorescence images were taken using a high pressure mercury arc light source.

Cell spreading and protrusive activity analysis

We used the neuronal tetraspanin molecule stargazin to label the plasma membrane in our studies. Endogenous stargazin expression in heterologous cells is very low[27], and previous studies have shown that expression of fluorescent protein-tagged stargazin results in uniform labeling of the plasma membrane[28]. The RapR-Src constuct had a Y529F mutation in the C-term of Src that prevented regulation of RapR-Src by upstream signaling pathways. Cells expressing RapR-Src-Cerulean constructs, stagazin-mCherry and GFP-FRB were selected using epifluorescence imaging. Time-lapse movies were taken at 2 min time intervals. Image analysis was performed using Metamorph software. A binary mask of a cell was created based on Stargazin-mCherry images and used to assess cell area. To calculate the cell area change we divided the cell area at the given time point by the area of the same cell at the time point immediately prior to addition of rapamycin. The following number of cells were analyzed: 56 cells for RapR-Src, 47 cells for the kinase-dead mutant (D388R) of RapR-Src, 36 cells for the control without RapR-Src, 49 cells for the SH3 domain mutant (W118A) of RapR-Src, 57 cells for the myristoylation mutant (G2A) of RapR-Src, 39 cells for activation of the G2A mutant of RapR-Src at the plasma membrane with myristoylated FRB, 76 cells for the SH2 domain mutant (R175L) of RapR-Src, 73 cells for activation of the R175L mutant of Src in complex with FAK-FRB, 73 cells for activation of the R175L mutant of RapR-Src in complex with p130Cas. To calculate the protrusive activity of the cell we first calculated the sum of the areas associated with regions of the cell that undergo

local extensions between subsequent movie frames. We refer to this area as the protrusive area. Then to determine fold change in protrusive activity we divided the protrusive area during each time interval by the time averaged protrusive area before the addition of rapamycin. The following numbers of cells were analyzed: 31 cells for RapR-Src, 21 cells for the kinase-dead mutant (D388R) of RapR-Src, 36 cells for the control without RapR-Src, 49 cells for the SH3 domain mutant (W118A) of RapR-Src, 42 cells for the myristoylation mutant (G2A) of RapR-Src, 29 cells for activation of the G2A mutant of RapR-Src at the plasma membrane with myristoylated FRB, 49 cells for the SH2 domain mutant (R175L) of RapR-Src, 35 cells for activation of the R175L mutant of Src in complex with FAK-FRB, 44 cells for activation of the R175L mutant of RapR-Src in complex with p130Cas.

Filopodia analysis

To quantify filopodia dynamics from time-lapse movies, we used a computational method that allows accurate identification and tracking of all cellular protrusions for cells and protrusions of arbitrarily complex shape[29] (Supplementary Fig. 2). Briefly, the steps involved in the process include:

1. Mapping the cell outline onto a tree graph. In general, an arbitrary closed (non-self-intersecting) polygonal chain can be mapped to a tree graph using a medial axis transform (MAT)[30-33]. The branches of the tree emanate from a single point inside the cell (the root of the tree) and eventually reach each point of the cell boundary. Thus, every boundary point is connected to a common origin through a unique path on the graph that always remains inside the cell, regardless of the complexity of the cell shape (Supplementary Fig. 2a). The root can be defined as the cell center, but it does not coincide with the centroid. It coincides with the center of the largest possible circle that can be inscribed within the cell boundary.

2. Boundary profiling. Plotting the distance along each graph path from the root to the boundary as function of the boundary points provides a mechanisms for identifying protrusions. In this graph, the protrusion tips appear as local maxima (Supplementary Fig. 2c).

3. Filopodia detection. The path that starts at the protrusion tip and runs through the center of the protrusion can be used to calculate protrusion length, while the short branches from these central lines to the boundary provide a measure of the protrusion width. Filopodia are defined by specifying cut-off values for the width and length of the protrusions (Supplementary Fig. 2b). In this way, we make sure that the algorithm selects only thin filopodia-like protrusions.

4. Filopodia tracking. The skeleton segments from the previous step not only allow us to define filopodia, but also provide a reliable method for tracking these protrusions over time and quantify their dynamic behavior. One important improvement of the algorithm, made specifically for the presented here analysis, was to include automated differentiation of active (dynamic) filopodia from passive structures resulting from cell retraction. This modification allowed us to increase the accuracy of filopodia quantification by avoiding overestimation due to retraction fibers at the cell edge.

The following number of cells were analyzed: 23 cells for RapR-Src, 23 cells for kinase-dead mutant (D388R) of RapR-Src, 33 cells for the control without RapR-Src, 22 cells for SH3 domain mutant (W118A) of RapR-Src, 25 cells for myristoylation mutant (G2A) of RapR-Src, 18 cells for activation of G2A mutant of RapR-Src at the plasma membrane with myristoylated FRB, 23 cells for SH2 domain mutant (R175L) of RapR-Src, 26 cells for activation of R175L mutant of Src in complex with FAK-FRB, 22 cells for activation of R175L mutant of RapR-Src in complex with p130Cas.

Focal adhesion analysis

Analysis of focal adhesions was performed as previously described[16, 34]. To determine focal adhesion number and elongation after rapamycin addition, we first calculated the average value of the property across all identified adhesions in each image, producing a time-series for each time-lapse image set. Each time-series was normalized so that the value immediately before rapamycin addition was equal to one. The following number of cells were analyzed: 22 cells for RapR-Src, 18 cells for the kinase-dead mutant (D388R) of RapR-Src, 27 cells for the SH3 domain mutant (W118A) of RapR-Src, 15 cells for the myristoylation mutant (G2A) of RapR-Src, 21 cells for activation of the G2A mutant of RapR-Src at the plasma membrane with myristoylated FRB, 35 cells for the SH2 domain mutant (R175L) of RapR-Src, 20 cells for activation of the R175L mutant of Src in complex with FAK-FRB, 25 cells for activation of the R175L mutant of RapR-Src in complex with p130Cas.

Supplementary Material

Refer to Web version on PubMed Central for supplementary material.

Acknowledgments

We thank Betsy Clarke for help with figures, and are grateful to the National Institutes of Health for funding (R21CA159179 to AVK, and GM102924, GM094663 to KMH).

References

1. Thomas SM, Brugge JS. Cellular functions regulated by Src family kinases. Annu Rev Cell Dev Biol. 1997; 13:513–609. [PubMed: 9442882]
2. Frame MC. Src in cancer: deregulation and consequences for cell behaviour. Biochim Biophys Acta. 2002; 1602:114–130. [PubMed: 12020799]
3. Playford MP, Schaller MD. The interplay between Src and integrins in normal and tumor biology. Oncogene. 2004; 23:7928–7946. [PubMed: 15489911]
4. Cross FR, Garber EA, Pellman D, Hanafusa H. A short sequence in the p60src N terminus is required for p60src myristylation and membrane association and for cell transformation. Mol Cell Biol. 1984; 4:1834–1842. [PubMed: 6092942]
5. Buss JE, Kamps MP, Sefton BM. Myristic acid is attached to the transforming protein of Rous sarcoma virus during or immediately after synthesis and is present in both soluble and membrane-bound forms of the protein. Mol Cell Biol. 1984; 4:2697–2704. [PubMed: 6441887]
6. Dhar A, Shukla SD. Involvement of pp60c-src in platelet-activating factor-stimulated platelets. Evidence for translocation from cytosol to membrane. J Biol Chem. 1991; 266:18797–18801. [PubMed: 1717453]

7. Weernink PA, Rijksen G. Activation and translocation of c-Src to the cytoskeleton by both platelet-derived growth factor and epidermal growth factor. J Biol Chem. 1995; 270:2264–2267. [PubMed: 7530720]
8. Resh MD, Erikson RL. Highly specific antibody to Rous sarcoma virus src gene product recognizes a novel population of pp60v-src and pp60c-src molecules. J Cell Biol. 1985; 100:409–417. [PubMed: 2981886]
9. Calothy G, et al. The membrane-binding domain and myristylation of p60v-src are not essential for stimulation of cell proliferation. J Virol. 1987; 61:1678–1681. [PubMed: 3106650]
10. Brown MT, Cooper JA. Regulation, substrates and functions of src. Biochim Biophys Acta. 1996; 1287:121–149. [PubMed: 8672527]
11. Webb DJ, et al. FAK-Src signalling through paxillin, ERK and MLCK regulates adhesion disassembly. Nat Cell Biol. 2004; 6:154–161. [PubMed: 14743221]
12. Shin NY, et al. Subsets of the major tyrosine phosphorylation sites in Crk-associated substrate (CAS) are sufficient to promote cell migration. J Biol Chem. 2004; 279:38331–38337. [PubMed: 15247284]
13. Karginov AV, Ding F, Kota P, Dokholyan NV, Hahn KM. Engineered allosteric activation of kinases in living cells. Nat Biotechnol. 2010; 28:743–747. [PubMed: 20581846]
14. Karginov AV, Hahn KM. Allosteric activation of kinases: design and application of RapR kinases. Curr Protoc Cell Biol. 2011; Chapter 14:13. Unit 14. [PubMed: 22161545]
15. Kmiecik TE, Shalloway D. Activation and suppression of pp60c-src transforming ability by mutation of its primary sites of tyrosine phosphorylation. Cell. 1987; 49:65–73. [PubMed: 3103925]
16. Berginski ME, Vitriol EA, Hahn KM, Gomez SM. High-resolution quantification of focal adhesion spatiotemporal dynamics in living cells. PLoS One. 2011; 6:e22025. [PubMed: 21779367]
17. Bjorge JD, Jakymiw A, Fujita DJ. Selected glimpses into the activation and function of Src kinase. Oncogene. 2000; 19:5620–5635. [PubMed: 11114743]
18. Sandilands E, Brunton VG, Frame MC. The membrane targeting and spatial activation of Src, Yes and Fyn is influenced by palmitoylation and distinct RhoB/RhoD endosome requirements. J Cell Sci. 2007; 120:2555–2564. [PubMed: 17623777]
19. Kamps MP, Buss JE, Sefton BM. Mutation of NH2-terminal glycine of p60src prevents both myristoylation and morphological transformation. Proc Natl Acad Sci U S A. 1985; 82:4625–4628. [PubMed: 2991884]
20. Pellman D, Garber EA, Cross FR, Hanafusa H. Fine structural mapping of a critical NH2-terminal region of p60src. Proc Natl Acad Sci U S A. 1985; 82:1623–1627. [PubMed: 2984663]
21. Schaller MD, et al. Autophosphorylation of the focal adhesion kinase, pp125FAK, directs SH2-dependent binding of pp60src. Mol Cell Biol. 1994; 14:1680–1688. [PubMed: 7509446]
22. Nakamoto T, Sakai R, Ozawa K, Yazaki Y, Hirai H. Direct binding of C-terminal region of p130Cas to SH2 and SH3 domains of Src kinase. J Biol Chem. 1996; 271:8959–8965. [PubMed: 8621540]
23. Cary LA, Han DC, Polte TR, Hanks SK, Guan JL. Identification of p130Cas as a mediator of focal adhesion kinase-promoted cell migration. J Cell Biol. 1998; 140:211–221. [PubMed: 9425168]
24. Parsons JT, Horwitz AR, Schwartz MA. Cell adhesion: integrating cytoskeletal dynamics and cellular tension. Nat Rev Mol Cell Biol. 2010; 11:633–643. [PubMed: 20729930]
25. Gustavsson A, Yuan M, Fallman M. Temporal dissection of beta1-integrin signaling indicates a role for p130Cas-Crk in filopodia formation. J Biol Chem. 2004; 279:22893–22901. [PubMed: 15044442]
26. Dagliyan O, et al. Rational design of a ligand-controlled protein conformational switch. Proc Natl Acad Sci U S A. 2013; 110:6800–6804. [PubMed: 23569285]
27. Choi J, et al. Phosphorylation of stargazin by protein kinase A regulates its interaction with PSD-95. J Biol Chem. 2002; 277:12359–12363. [PubMed: 11805122]
28. Chen L, et al. Stargazin regulates synaptic targeting of AMPA receptors by two distinct mechanisms. Nature. 2000; 408:936–943. [PubMed: 11140673]

29. Tsygankov D, et al. CellGeo: A computational platform for the analysis of shape changes in cells with complex geometries. J Cell Biol. 2014; 204:443–460. [PubMed: 24493591]
30. Lee DT. Medial axis transformation of a planar shape. IEEE Trans Pattern Anal Mach Intell. 1982; 4:363–369. [PubMed: 21869050]
31. Blum H. A transformation for extracting new descriptors of shape. Proc Symp Models for the Perception of Speech and Visual Form. 1967:362–380.
32. Chin F, Snoeyink J, Wang CA. Finding the Medial Axis of a Simple Polygon in Linear Time. Discrete and Computational Geometry. 1999; 21:405–420.
33. Aichholzer O, Aigner W, Aurenhammer F, Hackl T, Jüttler B, Rabl M. Medial axis computation for planar free-form shapes. Computer-Aided Design. 2009; 41:339–349.
34. Wu C, et al. Arp2/3 is critical for lamellipodia and response to extracellular matrix cues but is dispensable for chemotaxis. Cell. 2012; 148:973–987. [PubMed: 22385962]

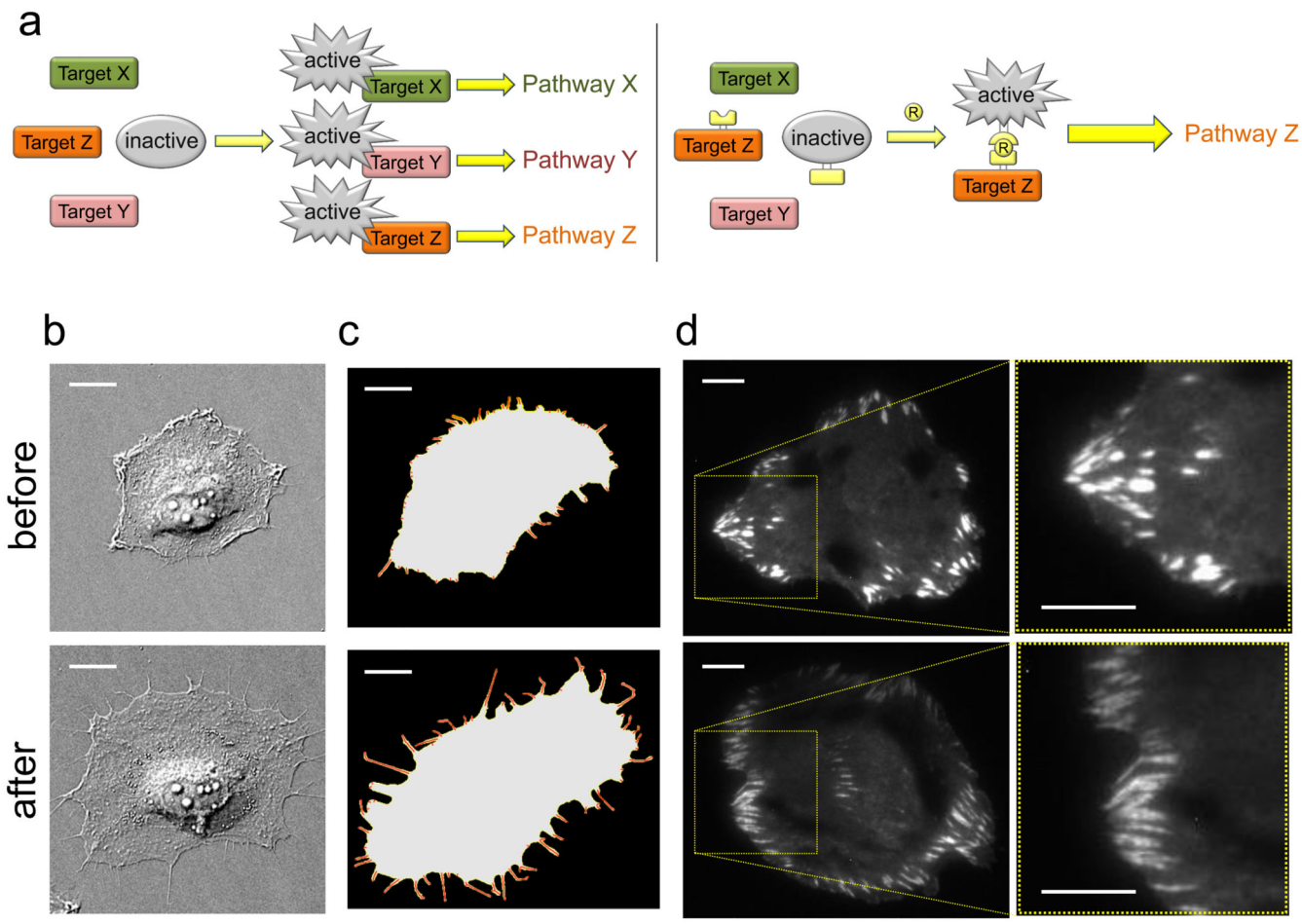

Fig. 1.

RapRTAP design and Src-induced morphological changes. (a) Unlike wild type kinases that are subject to complex upstream regulation and interact with multiple downstream targets (left), with RapR-TAP a specific kinase is activated to interact with only one specific target (right). Activation occurs when addition of rapamycin leads to interaction of two engineered domains (yellow), one on the kinase and the other on the target. (b-d) Before using RapRTAP to attribute specific roles to different Src interactions, the overall effects of Src were characterized by activating Src without targeting a specific effector protein. This produced: (b) spreading, (c) filopodia formation and lengthening, and (d) rearrangement of focal adhesions. Kinetics and quantitation of these phenotypes are shown in Supplementary Fig. 3-5. HeLa cells transiently co-expressing RapR-Src and FRB were imaged before and after addition of rapamycin. Cells were transiently co-transfected with mCherry-stargazin to visualize the cell membrane in (c), and with mCherry-paxillin to detect focal adhesions using TIRF microscopy in (d).

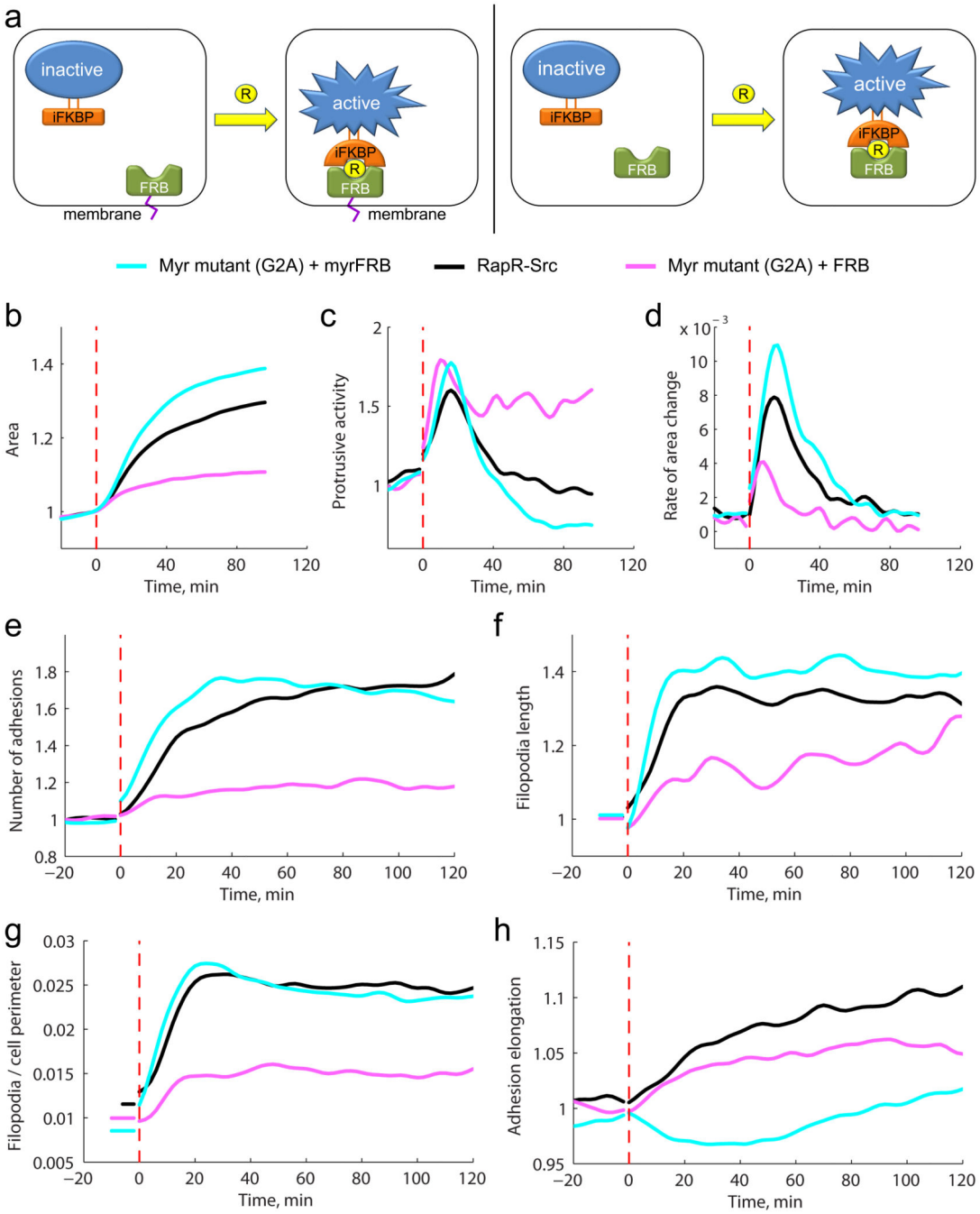

Fig. 2.

Restricting the activation of Src to specific subcellular locations. (a) The nonmyristoylated, cytoplasmic mutant of RapR-Src (G2A) was activated only when complexed with FRB. FRB that was membrane-anchored (left) versus free in cytoplasm (right) produced different Src-induced phenotypes. (b-h) Quantitative assays of phenotypes induced by Src activation (see methods and Supplementary Fig. 1, 2): cell spreading (b), protrusive activity (c) rate of area change (d), number of focal adhesions (e) filopodia length and number (f, g), and adhesion elongation (h). HeLa cells transiently co-expressing RapR-Src and FRB were

imaged every 2 minutes before and after addition of rapamycin. Membrane and adhesions were visualized as in Figure 1. Data are smoothed as a running average using a Gaussian filter. Unsmoothed data showing 90% confidence intervals is presented in Supplementary Fig. 10-15 (Number of cells analyzed: For RapR-Src area and rate of change 56, protrusive activity 31, filopodia 23, focal adhesion analysis 22; For G2A RapR-Src with FRB area and rate of area change 57, protrusive activity 42, filopodia 25, focal adhesion 15; For G2A RapR-Src with myristoylated FRB area and rate of area change 39, protrusive activity 29, filopodia 18, focal adhesions 21.)

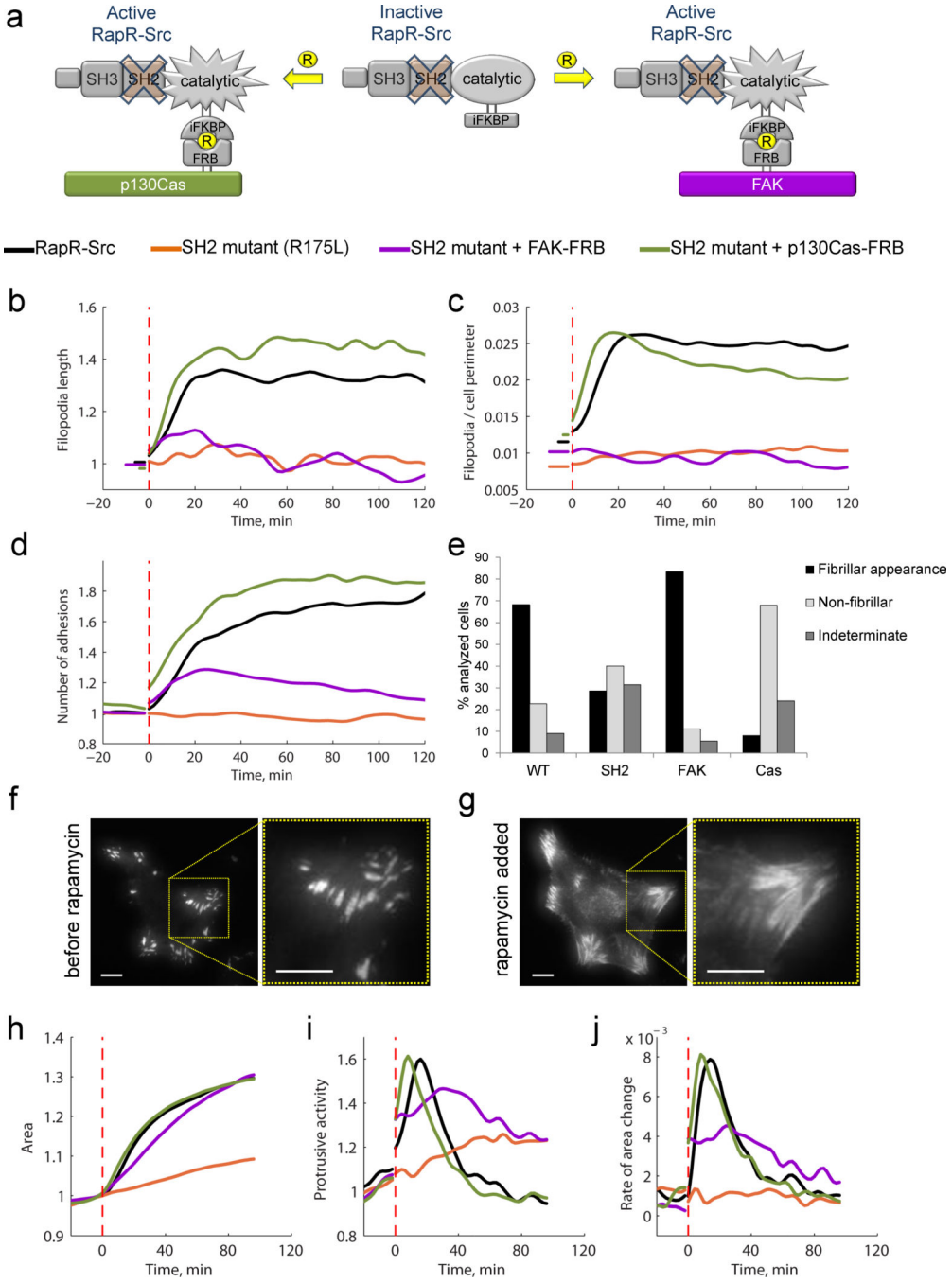

Fig. 3.

Activation of specific Src-protein complexes. (a) The Src SH2 mutant (R175L) interacted with either p130Cas or FAK only upon rapamycin addition. Activation was restricted to the target that bore FRB. (b-j) Effects on filopodia formation (b-c), adhesion formation and rearrangement (d-g), cell area (h, j) and protrusive activity (i). mCherry-tagged paxillin was used as a marker of focal adhesions. Analysis was performed as described in Fig. 2. Unsmoothed data showing 90% confidence intervals is presented in Supplementary Fig. 26-31. (Number of cells analyzed: For RapR-Src area and rate of change 56, protrusive

activity 31, filopodia 23, focal adhesion analysis 22; For SH2 mutant (R175L) area and rate of area change 76, protrusive activity 49, filopodia 23, focal adhesion 35; For SH2 mutant with FAK-FRB area and rate of area change 73, protrusive activity 35, filopodia analysis 26, focal adhesions 20; For SH2 mutant with p130Cas-FRB area and rate of area change 73, protrusive activity 44, filopodia 22, focal adhesions 25.)

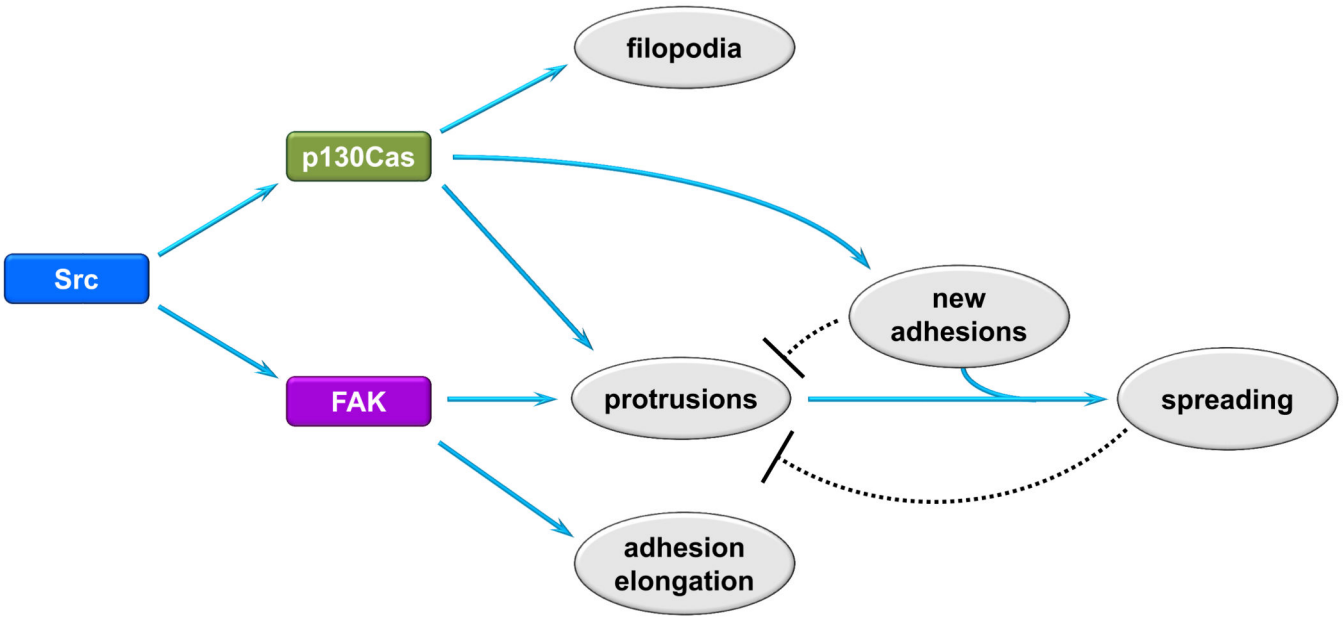

Fig. 4.

Model for the role of different Src-effector interactions. Src –p130Cas generates filopodia and Src-FAK causes adhesion elongation. Both Src-p130Cas and Src-FAK produce protrusion, but Src-FAK produces unceasing protrusion/retraction cycles with no stable increase in area, while Src-p130Cas generates cell spreading. Src-p130Cas is more effective at producing adhesions, potentially explaining the differences between protrusions induced by Src-FAK versus Src-p130Cas. Adhesion may enable protrusion to result in cell spreading, and feedback from adhesions may halt protrusive activity.